Title

Kelch-like Protein 11 Antibodies in Seminoma-Associated Paraneoplastic Encephalitis

Journal

New England Journal of Medicine, 381(1)

ISSN

0028-4793

Authors

Mandel-Brehm, Caleigh

Dubey, Divyanshu

Kryzer, Thomas J

et al.

Publication Date

2019-07-04

DOI

10.1056/nejmoa1816721

Peer reviewed

Published in final edited form as:

N Engl J Med. 2019 July 04; 381(1): 47–54. doi:10.1056/NEJMoa1816721.

Kelch-like Protein 11 Antibodies in Seminoma-Associated Paraneoplastic Encephalitis

Caleigh Mandel-Brehm, Ph.D.[#], **Divyanshu Dubey, M.D.**[#], **Thomas J. Kryzer, A.S.**, **Brian D. O'Donovan, Ph.D.**, **Baouyen Tran, Ph.D.**, **Sara E. Vazquez, B.S.**, **Hannah A. Sample, B.S.**, **Kelsey C. Zorn, M.H.S.**, **Lillian M. Khan, B.S.**, **Ian O. Bledsoe, M.D.**, **Andrew McKeon, M.D.**, **Samuel J. Pleasure, M.D., Ph.D.**, **Vanda A. Lennon, M.D., Ph.D.**, **Joseph L. DeRisi, Ph.D.**, **Michael R. Wilson, M.D.**[#], **Sean J. Pittock, M.D.**[#]

Department of Biochemistry and Biophysics (C.M.-B., B.D.O., S.E.V., H.A.S., K.C.Z., L.M.K., J.L.D.), the Weill Institute for Neurosciences (B.T., I.O.B., S.J. Pleasure, M.R.W.), the Department of Neurology (B.T., I.O.B., S.J. Pleasure, M.R.W.), and the Chan Zuckerberg Biohub (J.L.D.), University of California, San Francisco, San Francisco; and the Departments of Laboratory Medicine and Pathology (D.D., T.J.K., A.M., V.A.L., S.J. Pittock), Neurology (D.D., A.M., V.A.L., S.J. Pittock), and Immunology (V.A.L.), Mayo Clinic, Rochester, MN.

[#] These authors contributed equally to this work.

SUMMARY

A 37-year-old man with a history of seminoma presented with vertigo, ataxia, and diplopia. An autoantibody specific for kelch-like protein 11 (KLHL11) was identified with the use of programmable phage display. Immunoassays were used to identify KLHL11 IgG in 12 other men with similar neurologic features and testicular disease. Immunostaining of the patient's IgG on mouse brain tissue showed sparse but distinctive points of staining in multiple brain regions, with enrichment in perivascular and perimeningeal tissues. The onset of the neurologic syndrome preceded the diagnosis of seminoma in 9 of the 13 patients. An age-adjusted estimate of the prevalence of autoimmune KLHL11 encephalitis in Olmsted County, Minnesota, was 2.79 cases per 100,000 men.

Patients with autoimmune encephalitis may have specific serum autoantibodies and corresponding neurologic syndromes, associated neoplasms, and, in some cases, responsiveness to immunotherapies. Taken together, these features constitute recognizable syndromes.[1,2] Autoantibodies to Ma2, also known as anti-Ta, are a known marker for paraneoplastic brain-stem or limbic encephalitis associated with germ-cell tumors of the testis.[3–5] Patients have been described who have seminoma-associated paraneoplastic encephalitis but do not have IgG autoantibodies to Ma2 or to any other antigen and do not have specific immunofluorescence staining patterns on central nervous system tissue obtained from mice.[6–8]

Address reprint requests to Dr. Pittock at the Mayo Clinic, Department of Neurology, 200 First St. SW, Rochester, MN 55905, or at pittock.sean@mayo.edu.

Disclosure forms provided by the authors are available with the full text of this article at NEJM.org.

We describe a 37-year-old man (Patient 11) who underwent surgery to remove a testicular seminoma and received chemotherapy 3 years before the onset of progressive brain-stem and cerebellar encephalitis, or rhombencephalitis. Conventional paraneoplastic autoantibodies, including Ma2 IgG, were not detected. Using a customized phage display system,[9] we identified antibodies to the human protein kelch-like protein 11 (KLHL11) in this patient's cerebrospinal fluid. KLHL11 is a member of the E3 ubiquitin-protein ligase complex involved in protein ubiquitination.[10] The same antibody was detected in 12 other patients.

CASE REPORT

A left testicular seminoma (tumor–node–metastasis stage T2N0M0) was diagnosed in the patient at 32 years of age; he was treated with orchiectomy and a single cycle of carboplatin, and he was in remission for 45 months. Over a 9-month period, vertigo and truncal and appendicular ataxia developed; these conditions were complicated by diplopia 5 months before presentation. Examination 54 months after orchiectomy showed horizontal and vertical nystagmus with a rotatory component, intention tremor of the right arm with dysdiadochokinesia, dysmetria on finger–nose–finger testing on the right side, and a wide-based, cautious gait with impaired tandem gait. Magnetic resonance imaging (MRI) of the brain showed a nonenhancing hyperintense area adjacent to parts of the fourth ventricle on T_2-weighted images (Fig. S1A in the Supplementary Appendix, available with the full text of this article at NEJM.org). The cerebrospinal fluid contained 32 leukocytes per cubic millimeter, with a red-cell count of 11 per cubic millimeter, a protein concentration of 59 mg per deciliter, and a glucose concentration of 56 mg per deciliter (3.1 mmol per liter).

The patient's neurologic symptoms worsened, and he received intravenous methylprednisolone at a dose of 1 g daily for 5 days, followed by tapering doses of oral prednisone. Three weeks later, the truncal ataxia had improved and the eye-movement abnormalities, intention tremor, and dysmetria had resolved. He subsequently received intravenous immune globulin at a dose of 0.4 g per kilogram of body weight daily for 5 days and then monthly for 3 months. He received glatiramer acetate for a presumptive diagnosis of multiple sclerosis and had increasing ataxia over the next 8 months.

An MRI showed an enlarged and hyperintense left inferior olive on T_2-weighted images that did not enhance with the administration of gadolinium and was tentatively interpreted as a brainstem glioma (Fig. S1B in the Supplementary Appendix). The cerebrospinal fluid at that time contained 0 leukocytes per cubic millimeter, a red-cell count of 1 per cubic millimeter, protein concentration of 35 mg per deciliter, glucose concentration of 64 mg per deciliter (3.6 mmol per liter), and 14 oligoclonal bands that were not present in the serum (normal range, <2 oligoclonal bands). The reinitiation of high-dose glucocorticoid therapy led to resolution of the positional vertigo, and he received maintenance therapy with monthly intravenous immune globulin and rituximab.

At his initial evaluation, the patient was enrolled in a research study for detection of pathogens and autoantibodies. This study included antigen discovery by programmable phage display.[9] After identification of a candidate autoantigen, samples of the patient's serum and cerebrospinal fluid were evaluated to characterize the immunofluorescence

staining pattern. The immunofluorescence signal was sparse and punctate but was observed in several regions, including the hippocampus and brain stem, with enrichment in the perivascular tissue, perimeningeal tissue, and white-matter tracts (Fig. S2 in the Supplementary Appendix).

METHODS

The phage display was a modified human programmable display system (https://github.com/derisilab-ucsf/PhIP-PND-2018) engineered to screen for novel antigens.[9] Human cerebrospinal fluid or serum samples were incubated with 10^{10} plaque-forming units (PFU) per milliliter of a phage-display library, and antibody-bound phage particles were isolated by protein A and protein G immunoprecipitation. Antibody-bound phage particles were eluted, and DNA was sequenced to identify putative human antigen or antigens (Table S1 in the Supplementary Appendix). Putative novel antigens were validated with a human embryonic kidney (HEK) 293T–cell overexpression system, immunoprecipitation and Western blotting, mouse brain immunohistochemical analysis, or all of these methods.

The specificity of the IgG immunostaining pattern in the index patient and the additional patients described below was assessed qualitatively through comparison of the pattern yielded by IgG from 317 serum samples obtained from healthy controls, patients with cancer but no neurologic disease, and patients with other neurologic diseases, including paraneoplastic rhombencephalitis (in 42 patients). Of these 42 patients, 28 had anti–neuronal nuclear antibody type 2 (ANNA-2, or anti-Ri) IgG–associated brainstem encephalitis, 8 had Ma2 brain-stem encephalitis, and 6 had Purkinje cytoplasmic antibody type 1 (PCA-1, or anti-Yo)–associated paraneoplastic cerebellar degeneration (Table S2 in the Supplementary Appendix).

Full details of patient recruitment, methods pertaining to data collection, epidemiologic analysis, phage immunoprecipitation sequencing analysis, immunofluorescence assays on mouse brain tissue, and HEK 293T–cell overexpression assays are provided in the Methods section of the Supplementary Appendix.

ADDITIONAL PATIENTS

In assays conducted on mouse brain tissue, the immunofluorescence immunostaining pattern of samples obtained from the index patient was identical to that in 12 other patients who had been tested between 2001 and 2018 and whose information was retained in an archival series. All the patients had an encephalitic syndrome with brain-stem and cerebellar symptoms, and 10 had seminoma. All 13 patients with anti-KLHL11 encephalitis were men (Table 1). The median age at the onset of neurologic symptoms was 41 years (range, 27 to 68). The median titers of KLHL11 IgG antibodies in serum were 1:15,360 (range, 1:960 to 1:244,800; normal range, ≤1:120), and the median titers of KLHL11 IgG in cerebrospinal fluid were more than 1:712 (normal range, <1:2).

Eleven of the 13 patients presented with rhombencephalitis, in which ataxia was the most common initial symptom. One patient presented with cognitive decline, a mood disorder, hearing loss that was found by testing to be sensorineural, and trigeminal neuralgia. Other

neurologic symptoms included vertigo (in 8 of the 13 patients), hearing loss that was found by testing to be sensorineural (in 7), diplopia (in 6), and dysarthria (in 4). The cerebrospinal fluid samples in all patients had an elevated protein concentration, pleocytosis, oligoclonal bands, or an elevated IgG index. The median cerebrospinal fluid protein concentration was 69 mg per deci-liter (range, 30 to 93), and the median leukocyte count was 9 per cubic millimeter (range, 1 to 71, lymphocyte predominant). Initial MRI findings were mild cerebellar atrophy (in 6 patients), mid-brain hyperintensity on T_2-weighted images (in 1), cerebellar nuclei hyperintensity on T_2-weighted images (in 1), leptomeningeal enhancement (in 1), bilateral mesial temporal-lobe abnormalities (in 2), and normal (in 2).

Seminoma was identified in 11 patients (testicular in 8 and extratesticular in 3). The paraneoplastic neurologic syndrome led to testing that revealed the diagnosis of the tumor in 8 of the 11 patients. Two patients without seminoma had both testicular microlithiasis and fibrosis, putative premalignant conditions.[12–14] The median interval between the onset of neurologic symptoms and tumor diagnosis was 6 months (range, −42 to 158). Orchiectomy was performed in 10 patients, including the 2 patients with microlithiasis. Radiation therapy and chemotherapy (both in 5 of 11 patients) were also used to manage seminoma. All patients received immunotherapy to treat the neurologic syndrome (Table 1). One patient had sustained clinical improvement with the ability to walk independently, resolution of diplopia, and return to work, 8 patients had stabilization of the neurologic syndrome, and 4 had worsening of the neurologic syndrome after management of the underlying cancer or surgical removal of the microlithiasis and immunotherapy (Table 1).

Results of testing for KLHL11 antibodies in each patient (by means of phage display, immuno-precipitation, cell-based assay, and mouse brain immunohistochemical analysis) are listed in Table S1 in the Supplementary Appendix. The phage-display system identified KLHL11 as a putative autoantigen in the index patient (Patient 11), and this was confirmed in samples obtained from 7 additional patients from the immunofluorescence archival series (Fig. 1A). In this assay, antibodies from the cerebrospinal fluid or serum samples obtained from these patients, but not from healthy controls or patients with IgG auto-antibodies to Ma2, showed specific enrichment of KLHL11 protein–derived peptides (Fig. 1A). There was enrichment of a common peptide fragment within KLHL11 in the serum and cerebrospinal fluid of all the patients (Fig. S3 in the Supplementary Appendix).

The main findings were validated in vitro through immunoprecipitation of heterologously expressed full-length human KLHL11 from cerebrospinal fluid or serum samples from the patients (Fig. 1B). The other Ma2-negative patients (5 of 13 patients who were not tested by phage display) were identified as having anti-KLHL11 autoantibodies through cell-based assays and mouse brain immunohistochemical analysis. Figure 1C shows positive results on KLHL11 cell-based assays, and Figure 1D and 1E shows positive results on KLHL11 mouse brain immunohistochemical analysis.

We estimated the age- and sex-adjusted prevalence of paraneoplastic anti-KLHL11 encephalitis in Olmsted County, Minnesota, on the basis of the Rochester Epidemiology Project database from the Mayo Clinic, which contains the medical records of more than 95% of persons who lived in Olmsted County from January 1, 1966, to January 1, 2014.

This analysis resulted in an estimate of 1.4 cases per 100,000 population (95% confidence interval [CI], 0 to 3.3 per 100,000). The estimated age-adjusted prevalence among men was 2.79 cases per 100,000 population (95% CI, 0 to 6.65 per 100,000). The estimated incidence among men between January 1, 1995, and December 31, 2015, was 0.21 cases per 100,000 person-years (95% CI, 0 to 6.65 per 100,000).

DISCUSSION

We used comprehensive phage display to screen for novel autoantigens in an anti-Ma2–seronegative patient, and we detected a novel autoantigen, KLHL11.[9] We found this autoantigen in a cohort of clinically characterized patients who did not have anti-Ma2 autoantibodies and were identified retrospectively on the basis of a characteristic immunofluorescence pattern on mouse brain tissue, which was due to binding of patient antibodies to KLHL11. It is possible that the sparse immunofluorescence staining pattern we observed in anti-KLHL11 paraneoplastic encephalitis may have been overlooked in similar cases for which no immunofluorescence staining was identified.[6–8]

Most of the patients in this series presented with a syndrome of vertigo, tinnitus, hearing loss, and ataxia, and 11 of 13 had an underlying seminoma; 2 had testicular microlithiasis. The neurologic syndrome preceded the detection of cancer or a premalignant condition in 8 of 13 patients. In Olmsted County, KLHL11 IgG (estimated prevalence, 1.4 cases per 100,000 population) was rare, but the prevalence was higher than that of the other typical paraneoplastic antibodies associated with autoimmune encephalitis (e.g., ANNA2 IgG, 0.6 per 100,000 population; and collapsin response mediator protein 5 IgG, 0.7 per 100,000).[15]

Although rhombencephalitis has been reported among men with Ma2 IgG and testicular cancer, many Ma2 IgG–positive patients have clinical or imaging features that implicate the limbic system or diencephalon.[5] Other paraneoplastic brain-stem syndromes include those associated with ANNA-2, which differ from KLHL11 encephalitis in that they have different associated tumors, mainly carcinoma of the lung and breast, and clinical features including opsoclonus–myoclonus, laryngospasm, and jaw-opening dystonia that were not observed in the patients with KLH11 encephalitis.[16] Women with PCA-1 (anti-Yo)–associated paraneoplastic cerebellar degeneration can also present with a syndrome similar to KLHL11 encephalitis, but PCA-1 usually occurs with gynecologic and breast cancers.[17]

KLHL11 is one of 42 evolutionarily conserved proteins within the KLHL family that have in common a BACK (BTB and C-terminal kelch) domain, implicating a role in ubiquitination.[9] The epitope shared by all patients with KLHL11 in this study maps to the BACK domain within KLHL11 (Fig. S3 in the Supplementary Appendix). Autoantibodies specific for KLHL7 and KLHL12 have been reported in Sjögren's syndrome as well as in some cancers.[18–20] The intra-cellular localization of KLHL11 protein probably precludes a direct role of KLHL11 IgG in neuronal cell death and injury. In a similar manner to PCA-1 (anti-Yo) antibodies in paraneoplastic cerebellar degeneration, KLHL11 IgG may serve as a surrogate marker of a cytotoxic T-cell–mediated injury directed through T-cell receptors recognizing KLHL11 peptides.[17] Such a KLHL11-specific T-cell response may be stimulated by the lineage of KLHL11 IgG–producing B cells.[11]

In conclusion, we found that KLHL11 auto-antibodies were associated with paraneoplastic encephalitis in men with testicular cancer. Phage display was used to identify this novel paraneoplastic autoantibody.[9]

Supplementary Material

Refer to Web version on PubMed Central for supplementary material.

Acknowledgments

The content is solely the responsibility of the authors and does not necessarily represent the official views of the National Institutes of Health.

Supported by an award (R01AG034676) from the Rochester Epidemiology Project, which is funded by the National Institute on Aging of the National Institutes of Health; a grant (to Dr. DeRisi) from the Chan Zuckerberg Biohub; a grant (to Dr. Wilson) from the Rachleff Foundation; a grant (to Drs. Wilson, DeRisi, and Pleasure) from the University of California, San Francisco, Marcus Program in Precision Medicine Innovation; a grant (to Drs. Wilson, DeRisi, Mandel-Brehm, Pleasure, O'Donovan, and Tran, Ms. Sample, Ms. Zorn, and Ms. Kahn) from the University of California, San Francisco, Center for Next-Gen Precision Diagnostics, with funding from the Sandler Foundation and the William K. Bowes, Jr. Foundation; a Mentored Clinical Scientist Development Award (K08NS096117, to Dr. Wilson) from the National Institute of Neurological Disorders and Stroke; and a grant (to Drs. Dubey, McKeon, and Pittock) from the Center for Multiple Sclerosis and Autoimmune Neurology, Mayo Clinic.

We thank Carin Y. Smith and Sandra C. Bryant, M.S., for statistical support, Jessica A. Sagen, M.A., Patrick C. Andrews, B.S., James Fryer, M.S., and James B. Thoreson, A.S., for technical support, Mary J. Curtis for secretarial assistance, and the patients and their families for participation in this study.

Funded by the Rochester Epidemiology Project and others.

References

1. Graus F, Titulaer MJ, Balu R, et al. A clinical approach to diagnosis of autoimmune encephalitis. Lancet Neurol 2016; 15: 391–404. [PubMed: 26906964]
2. Tobin WO, Pittock SJ. Autoimmune neurology of the central nervous system. Continuum (Minneap Minn) 2017; 23: (3, Neurology of Systemic Disease): 627–53. [PubMed: 28570322]
3. Voltz R, Gultekin SH, Rosenfeld MR, et al. A serologic marker of paraneoplastic limbic and brain-stem encephalitis in patients with testicular cancer. N Engl J Med 1999; 340: 1788–95. [PubMed: 10362822]
4. Hoffmann LA, Jarius S, Pellkofer HL, et al. Anti-Ma and anti-Ta associated paraneoplastic neurological syndromes: 22 newly diagnosed patients and review of previous cases. J Neurol Neurosurg Psychiatry 2008; 79: 767–73. [PubMed: 18223018]
5. Dalmau J, Graus F, Villarejo A, et al. Clinical analysis of anti-Ma2-associated encephalitis. Brain 2004; 127: 1831–44. [PubMed: 15215214]
6. Ishikawa H, Kawada N, Taniguchi A, et al. Paraneoplastic neurological syndrome due to burned-out testicular tumor showing hot cross-bun sign. Acta Neurol Scand 2016; 133: 398–402. [PubMed: 26248690]
7. Freifeld Y, Kapur P, Chitkara R, Lee F, Khemani P, Bagrodia A. Metastatic "burned out" seminoma causing neurological paraneoplastic syndrome — not quite "burned out". Front Neurol 2018; 9: 20. [PubMed: 29441039]
8. van de Warrenburg BP, Rodriguez-Justo M, Vella NR, Freeman A, Bhatia KP, Quinn NP. Paraneoplastic cerebellar ataxia due to burnt-out testicular germ cell tumour? Eur Neurol 2007; 57: 178–81. [PubMed: 17218768]
9. Larman HB, Zhao Z, Laserson U, et al. Autoantigen discovery with a synthetic human peptidome. Nat Biotechnol 2011; 29: 535–41. [PubMed: 21602805]

10. Dhanoa BS, Cogliati T, Satish AG, Bruford EA, Friedman JS. Update on the Kelch-like (KLHL) gene family. Hum Genomics 2013; 7: 13. [PubMed: 23676014]
11. Robson NC, Donachie AM, Mowat AM. Simultaneous presentation and cross-presentation of immune-stimulating complex-associated cognate antigen by antigen-specific B cells. Eur J Immunol 2008; 38: 1238–46. [PubMed: 18398931]
12. Derogee M, Bevers RF, Prins HJ, Jonges TG, Elbers FH, Boon TA. Testicular micro-lithiasis, a premalignant condition: prevalence, histopathologic findings, and relation to testicular tumor. Urology 2001; 57: 1133–7. [PubMed: 11377326]
13. Dhankar SS, Agarwal RK, Kant K, Dewal DS. Seminoma in atrophic testis (report of 3 cases with review of literature). J Postgrad Med 1985; 31: 115–7. [PubMed: 2865368]
14. Wang T, Liu L, Luo J, Liu T, Wei A. A meta-analysis of the relationship between testicular microlithiasis and incidence of testicular cancer. Urol J 2015; 12: 2057–64. [PubMed: 25923148]
15. Dubey D, Pittock SJ, Kelly CR, et al. Autoimmune encephalitis epidemiology and a comparison to infectious encephalitis. Ann Neurol 2018; 83: 166–77. [PubMed: 29293273]
16. Pittock SJ, Lucchinetti CF, Lennon VA. Anti-neuronal nuclear autoantibody type 2: paraneoplastic accompaniments. Ann Neurol 2003; 53: 580–7. [PubMed: 12730991]
17. Albert ML, Darnell JC, Bender A, Francisco LM, Bhardwaj N, Darnell RB. Tumor-specific killer cells in paraneoplastic cerebellar degeneration. Nat Med 1998; 4: 1321–4. [PubMed: 9809559]
18. Ito K, Fujita T, Akada M, et al. Identification of bladder cancer antigens recognized by IgG antibodies of a patient with metastatic bladder cancer. Int J Cancer 2004; 108: 712–24. [PubMed: 14696098]
19. Stefanini GF, Bercovich E, Mazzeo V, et al. Class I and class II HLA antigen expression by transitional cell carcinoma of the bladder: correlation with T-cell infiltration and BCG treatment. J Urol 1989; 141: 1449–53. [PubMed: 2657113]
20. Uchida K, Akita Y, Matsuo K, et al. Identification of specific autoantigens in Sjögren's syndrome by SEREX. Immunology 2005; 116: 53–63. [PubMed: 16108817]

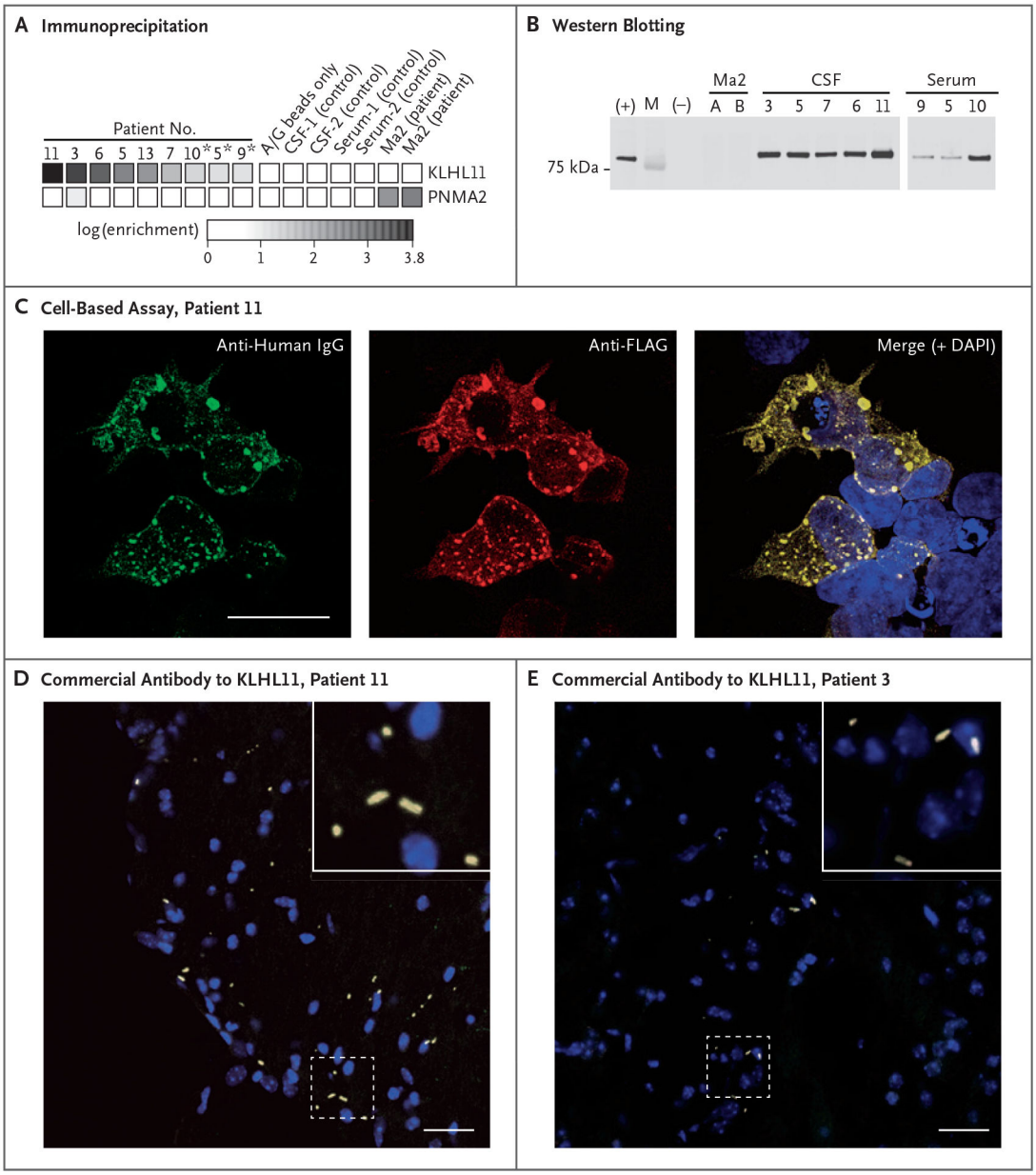

Figure 1. Discovery and Orthogonal Validation of Anti-KLHL11 Antibodies in Serum Samples Obtained from Men with Paraneoplastic Rhombencephalitis.

Panel A shows immunoprecipitation from a human phage display (10^{10} plaque-forming units [PFU] per milliliter) in cerebrospinal fluid (CSF) or serum samples (asterisks) obtained from the patients and healthy controls. Ma2 protein antigen (PNMA2) was identified in patients with encephalitis and autoantibodies to Ma2, and kelch-like protein 11 (KLHL11) antigen was identified in patients with novel, anti-Ma2–negative, seminoma-associated paraneoplastic encephalitis. Panels B through E show orthogonal validation of KLHL11 autoantibodies. Panel B shows detection of immunoprecipitated KLHL11 by Western blotting with an anti-FLAG antibody. KLHL11–MYC–FLAG was successfully immunoprecipitated by the serum or CSF IgG obtained from patients with autoimmune KLHL11 encephalitis (Patients 3, 5, 6, 7, 9, 10, and 11) and by a commercial antibody to KLHL11

(+), but not by the IgG of patients with anti-Ma2–associated encephalitis (Patients A and B) or protein A/G–negative controls (−). M denotes the protein marker. Panel C shows colocalization of the immunofluorescence signal from the IgG of Patient 11 (left) and anti-FLAG antibody (middle) in a cell-based assay with KLHL11–MYC–FLAG overexpression. The scale bar corresponds to 10 μm. Panels D and E show colocalization of the immunofluorescence signal from the KLHL1 IgG of Patient 11 (Panel D) and Patient 3 (Panel E) with a commercial antibody to KLHL11 on mouse brain tissue. The insets in Panels D and E show the degree of red and green channel overlap, or "yellow" signal at a higher magnification. (Areas represented in the insets are shown with dashed lines.) The scale bars correspond to 50 μm. Validation experiments in Panels B and C were completed with the use of the HEK293T cell overexpression system. For microscopy in Panels C through E, cell nuclei were identified with the use of DAPI (4′,6-diamidino-2-phenylindole) stain.

Table 1.

Clinical Features of Men with Novel Anti-KLHL11 Seminoma–Associated Paraneoplastic Encephalitis.*

Patient No. (Age at Symptom Onset)	Initial Symptoms	Diagnostic Tests and Results	Testicular Disease[11]	Immunotherapy	Clinical Course†	Months of Follow-up	Persistent Neurologic Deficits on Last Follow-up
1 (65 yr)	Vertigo, diplopia, sensorineural hearing loss, ataxia	CSF: 10 white cells/mm^3, protein, 40 mg/dl, 2 OCBs; Scrotal ultrasonography: right testicular mass	Stage IIIA testicular seminoma	Intravenous immune globulin, intravenous methylprednisolone	Stabilization	95	Bilateral sensorineural hearing loss, ataxia, diplopia
2 (51 yr)	Vertigo, diplopia, tinnitus, sensorineural hearing loss, ataxia	CSF: 17 white cells/mm^3, protein, 82 mg/dl, 14 OCBs; Scrotal ultrasonography: testicular mass	Stage I testicular seminoma	Intravenous methylprednisolone, intravenous immune globulin, mycophenolate mofetil	Stabilization	84	Diplopia, cervical amyotrophy, wide-based gait, ambulating with cane
3 (45 yr)	Diplopia, ataxia, seizures	CSF: 49 white cells/mm^3, protein, 93 mg/dl; Scrotal ultrasonography: atrophic testes and microlithiasis	Testicular fibrosis and microlithiasis	Intravenous immune globulin, intravenous methylprednisolone, mycophenolate mofetil, cyclophosphamide	Stabilization	59	Nystagmus, ataxia
4 (28 yr)	Vertigo, diplopia, sensorineural hearing loss, ataxia	CSF: 35 white cells/mm^3, protein, 86 mg/dl; Abdominal CT: intrapelvic mass	Stage IIIA testicular seminoma	Intravenous methylprednisolone, intravenous immune globulin, cyclophosphamide	Stabilization	60	Ataxia, wheelchair-dependent
5 (43 yr)	Vertigo, sensorineural hearing loss, ataxia	CSF: 1 white cell/mm^3, protein, 62 mg/dl, 6 OCBs; Chest CT: anterior mediastinal mass	Extratesticular seminoma (primary mediastinal extragonadal germ-cell tumor)	Intravenous methylprednisolone, cyclophosphamide	Improvement	98	Sensorineural hearing loss (right side), intermittent diplopia
6 (36 yr)	Visuospatial disorientation, memory loss, suicidal ideation, sensorineural hearing loss, trigeminal neuropathy	CSF: 7 white cells/mm^3, protein, 76 mg/dl, 9 OCBs; Scrotal ultrasonography: testicular mass	Stage IIA testicular seminoma	Intravenous methylprednisolone	Stabilization	216	Dementia, sensorineural hearing loss, trigeminal neuropathy
7 (29 yr)	Vertigo, diplopia, sensorineural hearing loss, ataxia	CSF: 8 white cells/mm^3, protein, 69 mg/dl, 3 OCBs; Chest CT: anterior mediastinal mass	Stage IIIAextratesticular seminoma	Intravenous immune globulin, intravenous methylprednisolone, rituximab, cyclophosphamide	Progressive decline	60	Diplopia, dysarthria, ataxia, paraplegia
8 (42 yr)	Dysarthria, ataxia	CSF: 3 white cells/mm^3, protein, 70 mg/dl; Scrotal ultrasonography: microlithiasis	Testicular fibrosis and microlithiasis	Intravenous methylprednisolone, intravenous immune globulin, rituximab, cyclophosphamide, natalizumab	Progressive decline	26	Dysarthria, ataxia, ambulation with walker

Patient No. (Age at Symptom Onset)	Initial Symptoms	Diagnostic Tests and Results	Testicular Disease[11]	Immunotherapy	Clinical Course[†]	Months of Follow-up	Persistent Neurologic Deficits on Last Follow-up
9 (68 yr)	Vertigo, sensorineural hearing loss, ataxia	CSF: 1 white cell/mm^3, protein, 43 mg/dl, 4 OCBs; Abdominal CT: retroperitoneal mass	Stage IIIB testicular seminoma	Intravenous methylprednisolone, cyclophosphamide	Progressive decline	8	Nystagmus, dysarthria, ataxia, wheelchair-dependent
10 (41 yr)	Dysarthria, ataxia, headaches	CSF: 71 white cells/mm^3, protein, 85 mg/dl; Whole-body PET-CT: hypermetabolic left periaortic lymph nodes	Stage IIAextratesticular seminoma	Intravenous methylprednisolone, plasma exchange, prednisone, rituximab, cyclophosphamide	Stabilization	14	Dysarthria, tinnitus, ataxia, wheelchair-dependent
11, index (37 yr)	Vertigo, diplopia, ataxia	CSF: 32 white cells/mm^3, protein, 59 mg/dl, 14 OCBs; Scrotal ultrasonography: left testicular mass	Stage I testicular seminoma	Intravenous methylprednisolone, intravenous immune globulin, rituximab	Progressive decline	43	Nystagmus, dysarthria, diplopia, ataxia, ambulation with walker
12 (40 yr)	Vertigo, dysarthria, ataxia	CSF: 9 white cells/mm^3, protein, 50 mg/dl, 9 OCBs; Scrotal ultrasonography: right testicular mass	Stage IIA testicular seminoma	Intravenous methylprednisolone, intravenous immune globulin, plasma exchange, prednisone, cyclophosphamide	Stabilization	10	Spasticity, ataxia, ambulation with cane
13 (27 yr)	Dysarthria, left upper-extremity tremor, imbalance	CSF: 2 white cells/mm^3, protein, 30 mg/dl, 10 OCBs; Scrotal ultrasonography: left testicular mass	Stage I testicular seminoma	Intravenous methylprednisolone, prednisone, intravenous immune globulin	Stabilization	2	Dysarthria, ataxia, visual fixation difficulties

[*] Patients are listed in chronological order according to the date of detection of a unique immunofluorescence pattern. CSF denotes cerebrospinal fluid, CT computed tomography, OCB oligoclonal band, and PET positron-emission tomography.

[†] Stabilization indicates that the patient's neurologic deterioration stopped and his condition was considered to be stable over the follow-up period.

N Engl J Med. Author manuscript; available in PMC 2020 January 04.